

Article

## Microwave-Assisted Routes for the Synthesis of Complex Functional Oxides

Jesús Prado-Gonjal <sup>1,2</sup>, Rainer Schmidt <sup>3</sup> and Emilio Morán <sup>1,\*</sup>

<sup>1</sup> Departamento Química Inorgánica I, Facultad de Ciencia Químicas, Universidad Complutense, 28040 Madrid, Spain; E-Mail: jpradogonjal@quim.ucm.es

<sup>2</sup> Department of Chemistry, University of Reading, Whiteknights, Reading RG6 6AD, UK

<sup>3</sup> Departamento Física Aplicada III, Grupo de Física de materiales Complejos (GFMC), Facultad de las Ciencias Físicas, Universidad Complutense, 28040 Madrid, Spain; E-Mail: rainer.schmidt@fis.ucm.es

\* Author to whom correspondence should be addressed; E-Mail: emoran@quim.ucm.es; Tel.: +34-91-394-4234; Fax: +34-91-394-4352.

Academic Editor: Cristina Leonelli

Received: 26 February 2015 / Accepted: 29 April 2015 / Published: 12 May 2015

---

**Abstract:** The synthesis of complex functional inorganic materials, such as oxides, can be successfully performed by using microwave irradiation as the source of heat. To achieve this, different routes and set-ups can be used: microwave-assisted synthesis may proceed in the solid state or in solution, aqueous or not, and the set ups may be as simple and accessible as domestic oven or quite sophisticated laboratory equipment. An obvious advantage of this innovative methodology is the considerable reduction in time—minutes rather than hours or days—and, as a consequence, energy saving. No less important is the fact that the particle growth is inhibited and the broad variety of different microwave or microwave-assisted synthesis techniques opens up opportunities for the preparation of inorganic nanoparticles and nanostructures. In this work, various microwave synthesis techniques have been employed: solid-state microwaves, single-mode microwaves using a TE<sub>10p</sub> cavity and microwave-assisted hydrothermal synthesis. Relevant examples are presented and discussed.

**Keywords:** microwave synthesis; inorganic materials; oxides; nanoparticles

---

## 1. Introduction

There is a permanent stimulus for searching alternative synthetic routes for inorganic materials. The so-called “Soft Chemistry” methods appeared in the 1970s, pioneered by Rouxel and Livage, where the reactions are performed at moderate temperature, preferably at room temperature but always below 500 °C [1]. The term “Soft Chemistry” has historically been used to describe several types of low-temperature solid-solid transformations such as intercalation/deintercalation, ion exchange, hydrolysis and redox reactions. A common feature of soft chemical reactions is the possibility to produce metastable compounds [2,3].

In the last two decades, other classes of alternative synthesis methods for inorganic solids appeared: the so-called “Fast Chemistry” techniques [4,5], which enhance the diffusion rate of the ceramic precursors by several orders of magnitude, reaction time is shortened—and often lower reaction temperatures are feasible. Such techniques include combustion synthesis, sonochemistry, spark plasma sintering and the procedures that are the object of this work: microwave-assisted methods of synthesis.

Some of the “Fast Chemistry” processes, mainly microwave-assisted techniques, are understood to be more environmentally friendly, *i.e.*, requiring less energy than conventional processes. Taking into account the energy requirements of the process and finding ways to minimize the energy are important considerations in “Green chemistry” or “sustainable chemistry” [6,7].

Microwaves have wavelength of 1 m–1 mm, corresponding to wave frequencies between 0.3 and 300 GHz respectively. The wavelength at which industrial and domestic microwave apparatus operate is standardized to 12.25 cm (2.45 GHz), but other frequency allocations do exist. The most important contribution for microwave material heating may be the dipoles in the material following the alternate electromagnetic field associated to the microwave, *i.e.*, dipolar molecules, such as water, do rotate, the very fast changing electric field occurs  $2.4 \times 10^9$  times per second and the resistance to that movement generates a considerable amount of heat, but other contributions are also possible: Dielectric losses (conduction currents), magnetic heating, magnetic losses (induction currents) or second order effects (*i.e.*, formation of a plasma).

The preparation of inorganic materials by using different microwave techniques was shown to be fruitful from the compositional, structural, properties and applications points of view:

- A wide range of different structure-types can be prepared: perovskite [8–13], spinel [14,15], pyrochlore [16], fluorite [17,18] or one-dimensional structures [19,20] are some examples.
- The prepared materials show a wide range of functional properties: ferromagnetism [21], ferroelectricity [22,23], multiferroicity [24,25], thermoelectricity [26,27], lithium and oxygen ion conductivity [19,28,29].

The broad variety of different microwave or microwave-assisted synthesis techniques open up opportunities for the preparation of inorganic nanoparticles and nanostructures. This allows the possibility to tune the morphology, and the physical and chemical properties of nanoscale materials.

In this work, various microwave synthesis techniques have been employed: solid-state microwaves, single-mode microwaves using a TE<sub>10p</sub> cavity and microwave-assisted hydrothermal synthesis.

## 2. Solid-State Microwave Synthesis

The term “Solid-State Microwave Synthesis” refers to microwave irradiation of solid precursors. The synthetic procedure consists in mixing the precursors and packing them into a pellet, which is then deposited in an adequate crucible (usually porcelain, alumina or SiC) and placed in multimode microwave oven (often a domestic one).

The microwave field in oven-like multimode instruments is distributed in a chaotic manner. Due to reflections from the cavity walls, multiple modes of the electromagnetic waves interact with the cavity load (Figure 1). In these large cavities, the field density is low and therefore the applied microwave power has to be high in order to achieve short heating rates [30–32].

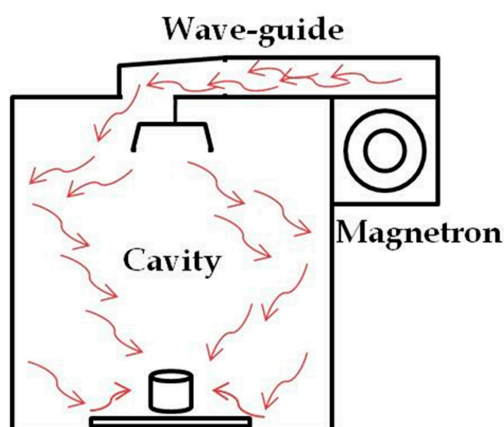


**Figure 1.** Schematic display of the field distribution in a multimode oven.

Due to the lack of temperature control in this type of microwave oven, the reactions are carried out at unknown temperature. However, the method has been applied to a large range of materials during the last years. Just a few examples are mentioned here to demonstrate the efficiency of the method for different types of materials.

### 2.1. $LaTMO_3$ ( $TM = Al, Cr, Mn, Fe, Co$ ) and $La_{1-x}Sr_xTMO_3$

Lanthanum perovskites containing metal oxides ( $LaMO_3$ ) of the first transition series are appealing functional materials because of their immense technological potential: some of them are used as components for solid oxide fuel cells (SOFCs), others are efficient catalysts, some are used as membranes for separation processes or as gas sensors in automobiles, several show magneto-optic or magnetoresistance properties. Moreover, some of these materials are multifunctional, in the case that different properties coexist [33–35].

All  $LaMO_3$  materials have been synthesized before by the traditional solid state method at high temperatures ( $>1000$  °C) for extended periods ( $>24$  h), and by means of other chemical methods, such as sol-gel, citrate complexation route, combustion, hydrothermal and sonochemistry, but their synthesis using microwave radiation in a reproducible way is scarce and just few authors have reported initial studies [36–39].

The equimolar amounts of metal nitrates were weighed according to the nominal composition of  $LaMO_3$  ( $M = Al, Cr, Mn, Fe, Co$ ) and mixed with 5% weight of carbon black, which can enhance

microwave absorption. The mixtures were mechanically homogenized and compacted in pellets of 12 mm diameter. The pellets were placed in a porcelain crucible, which were again placed inside another larger one stuffed with mullite and the whole setup was inserted into a domestic microwave oven [10].

LaCoO<sub>3</sub> and LaMnO<sub>3</sub> materials are directly obtained after 30 min of irradiation. On the other hand, LaAlO<sub>3</sub>, LaCrO<sub>3</sub> and LaFeO<sub>3</sub> need to be irradiated by microwaves for 30 min and heated afterwards in air in a conventional furnace for 2 h at specific temperatures (500 °C for LaFeO<sub>3</sub>, 800 °C for LaCrO<sub>3</sub> and 1000 °C for LaAlO<sub>3</sub>). To prepare doped materials such as La<sub>0.8</sub>Sr<sub>0.2</sub>FeO<sub>3</sub> and La<sub>0.8</sub>Sr<sub>0.2</sub>Fe<sub>0.5</sub>Co<sub>0.5</sub>O<sub>3</sub>, it is necessary to combine the described microwave method with the sol-gel methodology.

The more efficient heating mechanism in LaMnO<sub>3</sub> and LaCoO<sub>3</sub> may be explained by their metallic character. The first LaMnO<sub>3</sub> and LaCoO<sub>3</sub> clusters formed from the precursors may act in a similar way as the black carbon added, acting as a microwave susceptor: the first metallic clusters produced scatter the microwave radiation and higher temperatures may be reached quickly speeding up the reaction until completion. The microwave heating does not proceed in the same way for LaMO<sub>3</sub> ( $M = \text{Al, Cr, Fe}$ ), mainly due to their semiconducting character and an amorphous material is obtained after 30 min of microwave irradiation. Figure 2 shows an example of the X-ray diffraction pattern evolution for LaFeO<sub>3</sub>. On the other hand, for La<sub>0.8</sub>Sr<sub>0.2</sub>FeO<sub>3</sub> and La<sub>0.8</sub>Sr<sub>0.2</sub>Fe<sub>0.5</sub>Co<sub>0.5</sub>O<sub>3</sub>, the microwave heating proceeds in an even more complicated way as for the other samples and even longer times of microwave irradiation (up to 2 h) do not yield crystalline materials. Obviously, this synthetic route is not successful for doped LaMO<sub>3</sub> materials, and another intermediate step is necessary such as the preparation of a gel. In the Sr-doped variants we associate the less favorable microwave synthesis mechanism to the existence of secondary phases that may be difficult to get rid of.

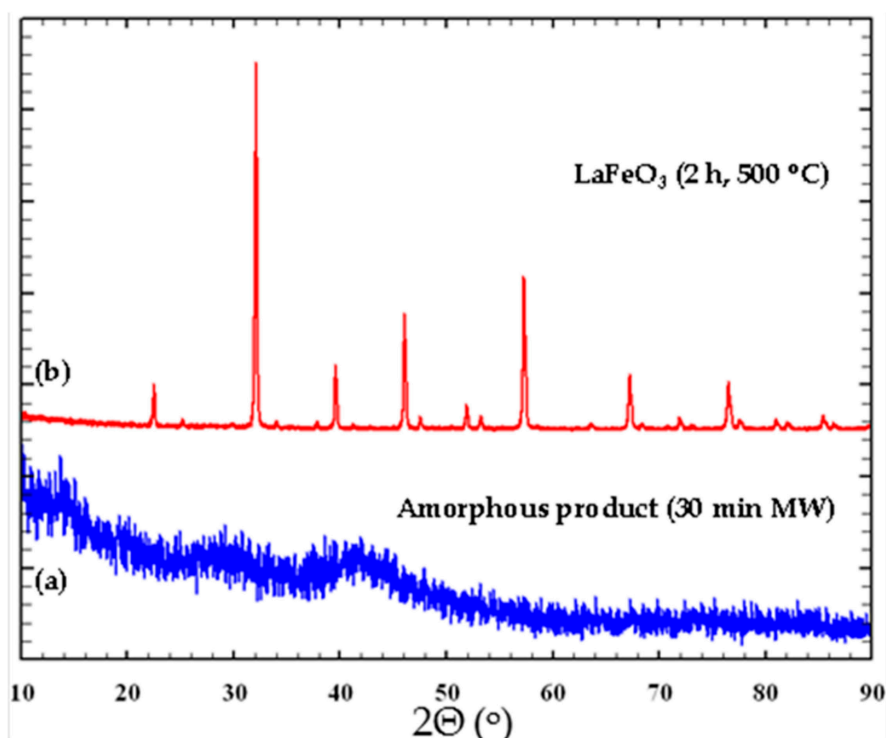


**Figure 2.** X-ray diffraction patterns of (a) Amorphous La-Fe-O product obtained after 30 min microwave irradiation (b) Crystalline LaFeO<sub>3</sub> synthesized after calcination of the previously amorphous powder during 2 h at 500 °C.

The XRD patterns of all binary  $\text{LaTMO}_3$  perovskites shown in Figure 3 exhibit the basic reflections corresponding to the perovskite structure and all Bragg reflections of the materials can be indexed by comparison with the respective JCPDS cards.  $\text{LaCrO}_3$ ,  $\text{LaMnO}_3$  and  $\text{LaFeO}_3$  crystallize in the  $Pnma$  space group and a displacement of the main peaks towards lower angles can be observed by comparison of the XRD patterns.

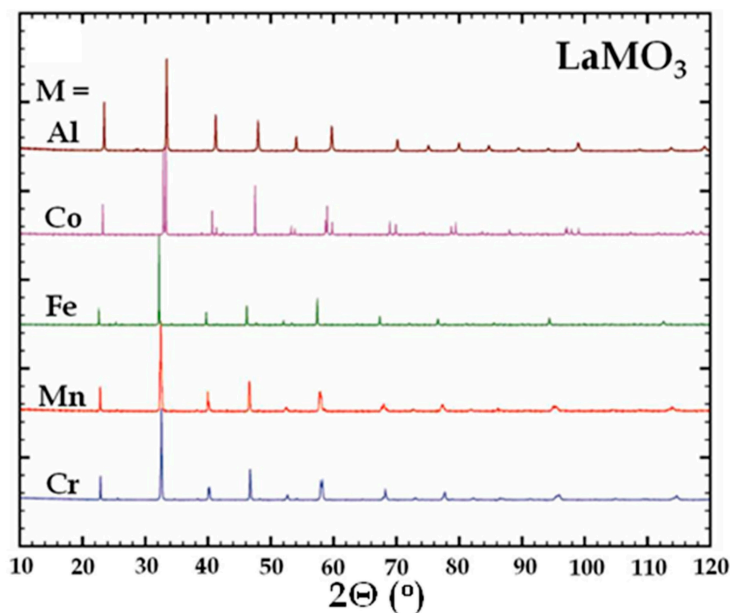


**Figure 3.** X-ray diffraction patterns of undoped lanthanum perovskites.

## 2.2. $(\text{RE})_2\text{Ti}_2\text{O}_7$ ( $\text{RE} = \text{Rare Earth}$ )

$\text{RE}_2\text{Ti}_2\text{O}_7$  pyrochlore oxide compounds are materials that can possess wide range functional properties such as ionic conductivity, exotic magnetic properties and multiferroic behavior. The crystal structure may be regarded a superstructure of oxygen deficient fluorite ( $\text{RE}_{0.5}\text{Ti}_{0.5}\text{O}_{1.75}$ ) with ordered  $\text{RE}^{3+}$  and  $\text{Ti}^{4+}$  cations, where an amount of 0.25 of the anions would be missing which allows ionic oxygen vacancy conduction to occur [40,41].

Traditionally,  $(\text{RE})_2\text{Ti}_2\text{O}_7$  compounds are prepared by solid state reaction, which requires long firing times (>1 day) with temperatures higher than  $1400^\circ\text{C}$  and intermediate grinding to achieve single phase material [42]. Alternatively, pyrochlores can be synthesized more rapidly using the respective metal nitrates in two steps: (1) 20 min microwave irradiation; (2) Calcination. This leads to a considerable reduction in calcination temperature ( $1100^\circ\text{C}$ ) and time (2 h).

Figures 4a,b show the SEM micrographs of different pyrochlore powders. The powders are composed by agglomerations of submicron and nanometric spherical particles, with high homogeneity and a sponge-like texture. This morphology is probably due to the big amount of gases produced during the synthesis from the decomposition of the starting nitrates and oxidation of the carbon microwave susceptor to  $\text{CO}_2$ . The small particle size may be adequate for processing ceramic materials with high sintering activity. After the sintering process ( $1400^\circ\text{C}$  during 4 h), the materials show high density and strongly increased particle size due to the high sintering activity of the initial powders as revealed in Figure 4c,d.

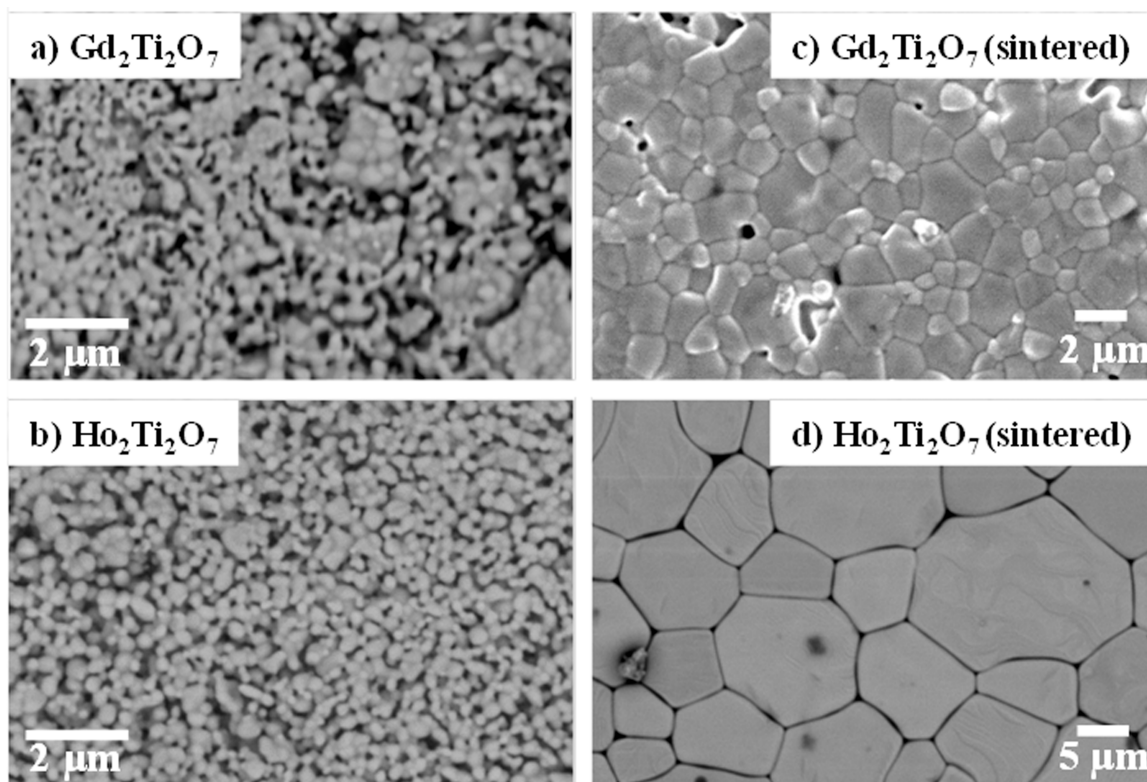


**Figure 4.** SEM micrographs of the RE<sub>2</sub>Ti<sub>2</sub>O<sub>7</sub> samples. (a,b) corresponds to Gd<sub>2</sub>Ti<sub>2</sub>O<sub>7</sub> and Ho<sub>2</sub>Ti<sub>2</sub>O<sub>7</sub> powder sample, respectively; (c,d) corresponds to pellets sintered at 1400 °C during 4 h.

### 3. Single-Mode Solid-State Microwave Synthesis (Using a TE<sub>10p</sub> Microwave Cavity)

Single-mode or monomode reactors can be considered as the second generation of microwave instruments, where the microwave utilized for heating is polarized and exhibits minima and maxima in the amplitude across the cavity. The electric and magnetic fields are well defined and stable in their spatial orientation, and the material to be heated needs to be placed at a certain position in the cavity for either electric or magnetic heating [43,44].

The single-mode microwave equipment used in this work is based on a microwave generator working at the standard 2.45 GHz frequency with a variable power up to 2 kW and a TE<sub>10p</sub> microwave cavity. The experimental set-up includes a microwave generator, circulator (water cooled magnetron), 3-stub tuner (impedance agreement accord) and the resonant cavity (Figure 5a). The amplitude distributions of the electric and magnetic components of the microwave can be utilized by carefully choosing the position of the sample during synthesis with respect to the respective maxima and minima of E and H (Figure 5b,c). By tuning the length of the cavity by moving a coupling iris and a short circuit piston it is possible to work in TE<sub>102</sub> or TE<sub>103</sub> resonant modes (Figure 5d,e). In the TE<sub>102</sub> mode the sample is placed at the amplitude maximum of the magnetic field component of the microwave (H mode), whereas in the TE<sub>103</sub> mode the sample is placed at the amplitude maximum of the E field (E mode) [45–47]. The reaction temperature is usually monitored with a pyrometer.

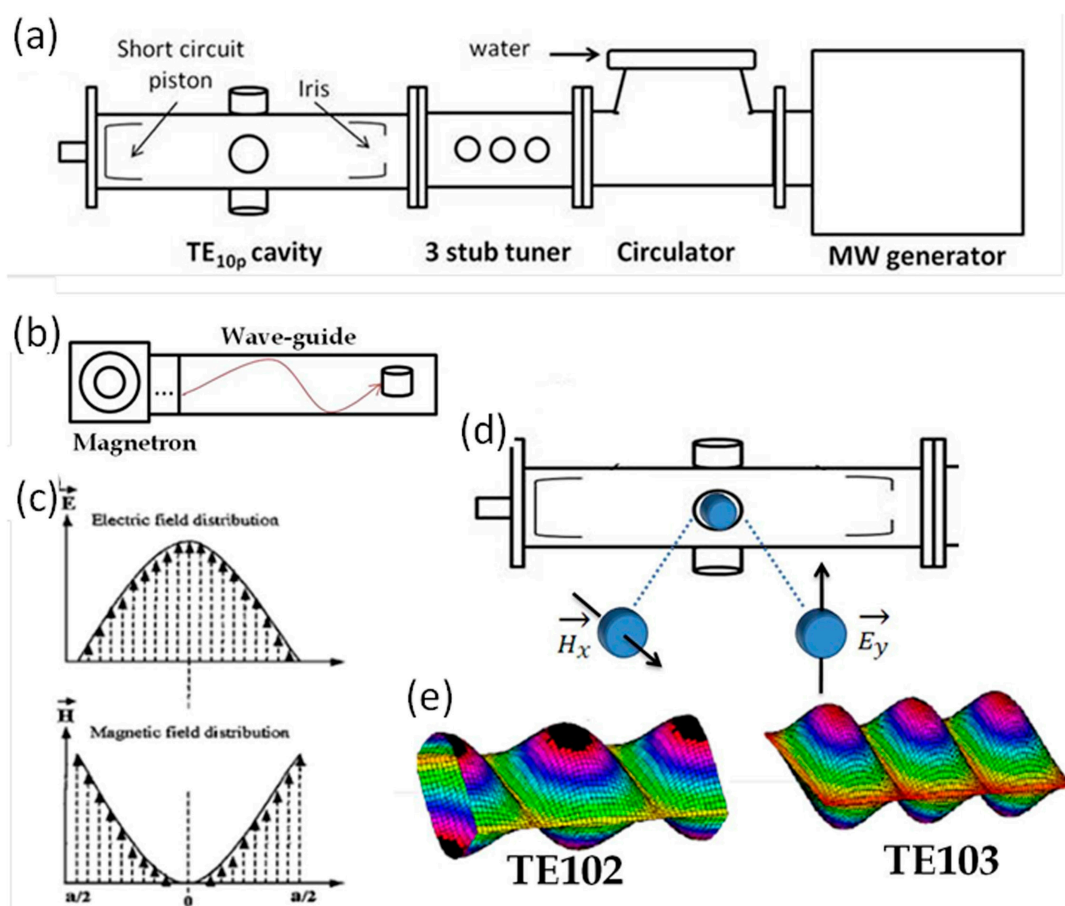


**Figure 5.** (a) Single-mode microwave apparatus (schematic picture); (b) Schematic display of a single-mode resonant cavity; (c) Amplitude distribution of the electromagnetic field: the sample is in the amplitude maximum of the electric  $E$  field where the magnetic field amplitude is minimum. Vice versa, the amplitude maximum of the magnetic  $H$  field corresponds to the minimum of the electric field  $E$ ; (d) Schematic drawing of the magnetic and electric field orientation of the polarized wave; (e) Amplitude distribution of the magnetic field component for the  $TE_{102}$  mode. For the  $TE_{103}$  mode the amplitude distribution of the electric field component is shown.

In general, conductive samples such as metals can be much more efficiently heated in the magnetic field. In contrast, ceramic insulators with low conductivity such as  $Al_2O_3$  and  $ZnO$  show much higher heating rates in the electric field. If ceramics and metals are combined (mixed systems), sample heating may be performed in both electric or magnetic fields [31,45]. This feature clearly indicates that for a complete understanding of the interaction between microwaves and matter it is necessary to consider the interactions of the electric and magnetic parts of the microwave with matter separately.

### 3.1. $Ba_xMn_8O_{16}$

$Ba_xMn_8O_{16}$  with hollandite structure is an appealing functional material in view of potential technological applications. This manganite is a mixed-valence compound with magnetic frustration due to the triangular framework and strong antiferromagnetic interactions. Furthermore, this material exhibits a semiconducting behavior [48,49].

To synthesize this complex material, a mixture of  $\text{Ba}(\text{NO}_3)_2$ ,  $\text{Mn}_2\text{O}_3$  and  $\text{KCl}$  (Sigma-Aldrich, Madrid, Spain) in a molar ratio of 1.2:4:12 was ground during 15 min in an agate mortar and pressed into pellets.  $\text{KCl}$  is added to the metal precursors as a mineralizer to avoid the formation of the perovskite phase  $\text{BaMnO}_3$ , which is in fact more stable than the hollandite phase. The pellet was placed into a SiC crucible. Only 5 min are sufficient to prepare this material in a single-mode microwave apparatus where the radiation is guided along a commercial  $\text{TE}_{10p}$  microwave cavity. The length of the microwave cavity was tuned to excite the  $\text{TE}_{102}$  mode for magnetic heating. The thermal cycle included a ramp of  $\approx 300\text{ }^\circ\text{C}/\text{min}$  and a dwell time of 5 min at  $900\text{ }^\circ\text{C}$ . The incident microwave power required to reach  $\approx 900\text{ }^\circ\text{C}$  is roughly 200 W. After the specific holding time at high temperature ( $900\text{ }^\circ\text{C}$ ), the microwave power was switched off and the sample cooled down to room temperature with a cooling ramp of  $\approx 300\text{ }^\circ\text{C}/\text{min}$ . The powder obtained was washed in distilled water to dissolve  $\text{KCl}$  and is dried afterwards in an oven at  $80\text{ }^\circ\text{C}$ . This route is much simpler and faster than the conventional procedure described in reference [48]: They heated the pellet in an alumina crucible up to  $850\text{ }^\circ\text{C}$  ( $100\text{ }^\circ\text{C}/\text{h}$ ), the holding time at  $850\text{ }^\circ\text{C}$  was 72 h, which was followed by another  $900\text{ }^\circ\text{C}$  treatment for 48 h in air after an intermediate grinding.

It is worth noting that the heating starts from the sample surface before propagating across the full sample in few seconds (see the sequence in Figure 6). This heat propagation mechanism is reminiscent to the auto-propagation front movement that occurs in fast chemistry combustion methods.

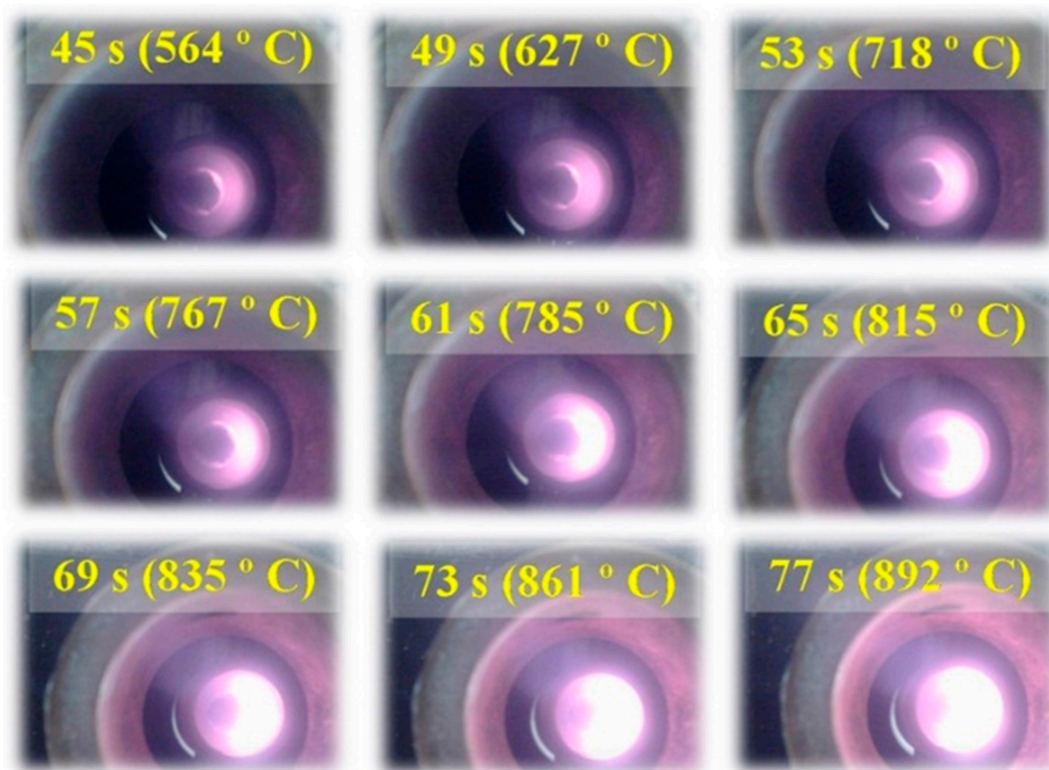


**Figure 6.** Sequence pictures of the single-mode microwave synthesis of  $\text{Ba}_x\text{Mn}_8\text{O}_{16}$ .

The phase structure and purity of the material were examined by X-ray diffraction (XRD). All diffraction peaks could be indexed according to the monoclinic phase  $\text{BaMn}_8\text{O}_{16}$   $I2/m$  (#12) (Figure 7).



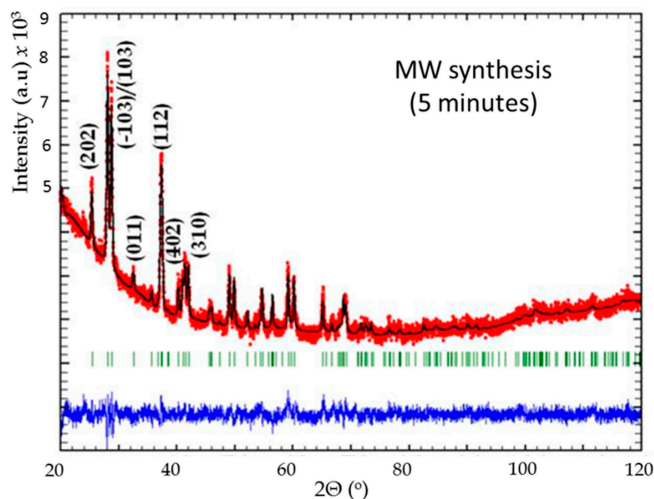


**Figure 7.** Rietveld refinement of powder X-ray diffraction patterns  $\text{Ba}_x\text{Mn}_8\text{O}_{16}$  from 5 min microwave irradiation: observed (red dotted lines), refined (black solid lines), and their difference (blue bottom line). Green vertical bars indicate the X-ray reflection positions.

### 3.2. $\text{LaCrO}_3$

$\text{LaCrO}_3$  perovskite has been widely recognized as promising interconnect material for SOFCs [50]. This material was synthesized by a single mode microwave equipment (SAIREM, Microwave Specialist Company, Cedex, France) in the TE102 mode (H mode) in just 2 min with a microwave power of 150 W, where the temperature was controlled to be about 900 °C. As mentioned above, the H mode may be less common for ceramic materials but is feasible here due to the  $\text{Cr}^{3+}$  magnetic structure providing sufficient magnetic losses. The starting precursors used were the metal nitrates in the appropriate stoichiometric ratio. The space group of the phase pure  $\text{LaCrO}_3$  obtained was the expected orthorhombic  $Pnma$ . X-ray diffraction Rietveld refinement is shown in Figure 8.

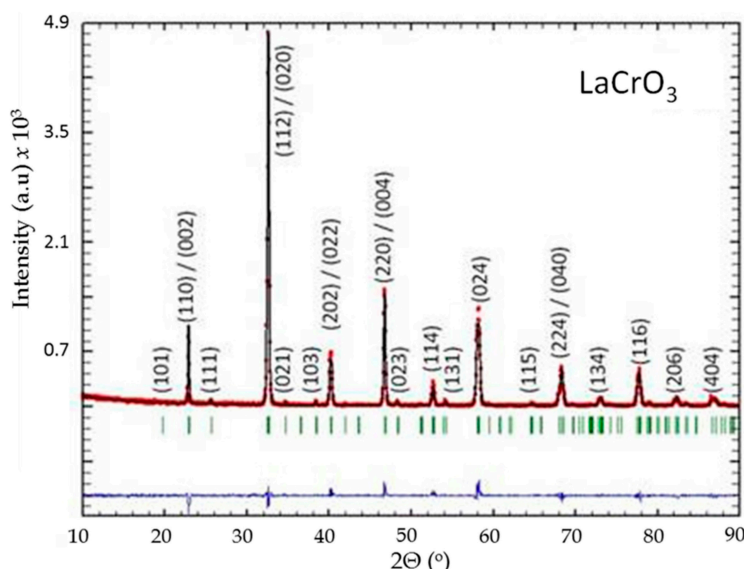


**Figure 8.** Rietveld refinement of powder X-ray diffraction patterns of  $\text{LaCrO}_3$ : observed (red dotted lines), refined (black solid lines), and their difference (blue bottom line). Green vertical bars indicate the X-ray reflection positions.

#### 4. Microwave-Assisted Hydrothermal Synthesis

The main difference between hydrothermal and solid-state reactions lies in the reactivity, which is reflected in their different reaction mechanisms. Solid state reactions depend on the diffusion of the raw materials at their interfaces, whereas in hydrothermal or solvothermal reactions the reactant ions and/or molecules react in solution. The difference of reaction mechanisms may lead to different microstructure of the products, even if the same reactants are used [51]. Although the hydrothermal method is versatile, one of the main drawbacks is slow kinetics of solution/crystallization at any given temperature.

In the early 1990s, Prof. Sridhar Komarneni at the University of Pennsylvania launched a pioneering work by studying and comparing the differences between hydrothermal syntheses performed with conventional means of heating and hydrothermal syntheses performed by heating pressure-sealed autoclaves with microwaves. In order to accelerate the kinetics of solution/crystallization, one may use microwaves for heating the solution due to the excellent coupling of the microwave to the polar water molecules in the solution [23,52,53].

Besides the characteristic microwave parameters of power and time, the method of microwave-assisted hydrothermal synthesis involves additional parameters such as the pH of the solution, the reaction temperature and pressure. Therefore, more advanced synthesis technology is required to control pressure and temperature in the subcritical region of water. A Milestone Ethos One microwave system has been used for the preparation of different functional materials.

##### 4.1. Rare Earth Doped—Cerium

Ceria-based solid solutions have been regarded promising candidates to serve as electrolytes in IT-SOFCs since their oxygen ion conductivities are higher than that of yttria stabilized zirconia YSZ in the intermediate temperature range (500–800 °C). Gadolinium and samarium-doped ceria have been extensively studied due to their high ionic oxygen conductivity [54,55].

Nano-sized particle powders can be synthesized by microwave-assisted hydrothermal synthesis at low reaction temperature (200 °C), where particle growth is minimized. Rare Earth nitrates (Sigma Aldrich, Madrid, Spain) and Potassium hydroxide KOH flakes, 90% (Sigma-Aldrich) were used as starting chemicals [29]. The aqueous solutions of each composition were prepared by dissolving the nitrate salt to the desired concentrations in distilled water and dilution in 1.2 M KOH under constant stirring. The solution was ultrasonically dispersed for 2 min and the reactions were carried out in double-walled vessels consisting of an inner Teflon sealed autoclave and an outer shell high strength polymer. The double-walled vessels were placed in the Milestone ETHOS 1 microwave system, which was operated at 2.45 GHz. The heating ramp up to 200 °C was set to  $\approx 12$  °C/min, the holding time at 200 °C was 30 min, which was followed by switching off the microwave power to furnace cool to room temperature at  $\approx 5$  °C/min. The reaction vessels were connected to a pressure transducer in order to monitor the autogenous pressure, which was found to amount to  $\approx 16$  bars during the 30 min holding time at 200 °C. The crystallized powders obtained were decanted 3 times, rinsed with distilled water to eliminate the remaining impurities and dried at 80 °C.

Figure 9 shows a TEM micrograph of  $\text{Ce}_{0.8}\text{Sm}_{0.18}\text{Ca}_{0.02}\text{O}_{1.9-\delta}$  powder, where it is clear that particles are nanosized (less than 20 nm) with only slight agglomerations. The corresponding SAED patterns

(insets of Figure 9) show the diffraction rings commonly observed in polycrystalline materials. Impedance spectroscopy measurements on sintered ceramics confirmed ionic charge transport in the microwave-synthesized rare-earth doped ceria [29].

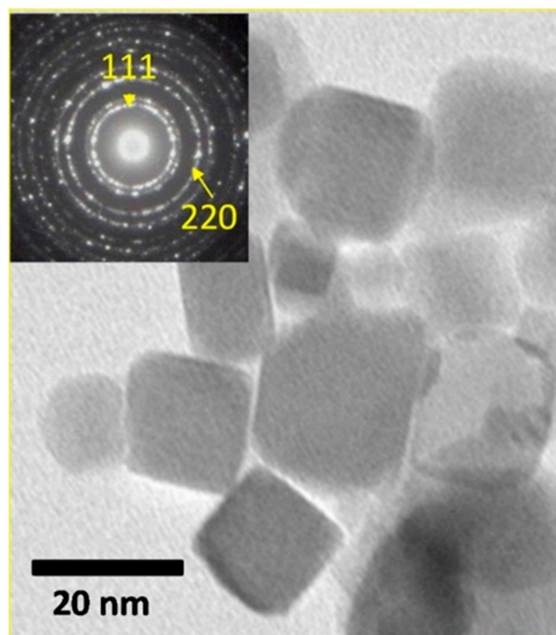


**Figure 9.** TEM micrograph of  $\text{Ce}_{0.8}\text{Sm}_{0.18}\text{Ca}_{0.02}\text{O}_{1.9-\delta}$  and in the top corners the SAED patterns.

#### 4.2. $\text{H}_2\text{V}_3\text{O}_8$

This material, also referred in the literature as  $\text{V}_3\text{O}_7 \cdot \text{H}_2\text{O}$ , has been reported to perform as cathode material for lithium intercalation with  $240 \text{ mAh} \cdot \text{g}^{-1}$  specific capacity, corresponding to the insertion of 2.5 Li per formula unit in the 4–1.5 V range. By using microwave-hydrothermal synthesis, an initial capacity of  $400 \text{ mAh} \cdot \text{g}^{-1}$  is developed in the 3.75–1.5 V range [19]. This is another clear example of an improved property after synthesizing a material using microwave irradiation.

The reaction was carried out in a quartz pressure vessel instead of Teflon autoclaves used in the other procedures described for doped-ceria. The convenience of using a quartz vessel is due to the high melting point of quartz material which will exclude possible damaged by localized superheating of the material inside the vessel. In the case of  $\text{H}_2\text{V}_3\text{O}_8$  and vanadium oxides, the possible formation of conducting phases can produce “hot spots” easily around the walls and the effect within a Teflon vessel would be catastrophic.

The reactants  $\text{V}_2\text{O}_5$  (0.5 mmol, Sigma Aldrich, Madrid, Spain, 98%) and ethanol (5 mL, Scharlau, Barcelona, Spain, synthesis grade) are mixed in 20 mL distilled water as solvent and placed and stirred in the vessel. The following optimized heating program was used: a heating ramp of  $12 \text{ }^\circ\text{C}/\text{min}$  up to  $200 \text{ }^\circ\text{C}$ , then 2 h holding time at  $200 \text{ }^\circ\text{C}$  followed by switching off the microwave. The SEM image displayed in Figure 10 shows the morphology of  $\text{H}_2\text{V}_3\text{O}_8$  nanobelts obtained using the microwave-hydrothermal route. They exhibit a width close to 100 nm and a length of several tens of micrometers.

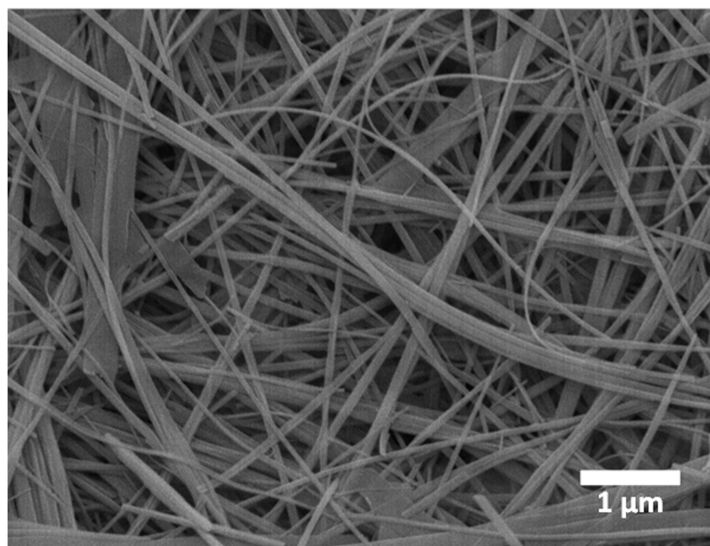


**Figure 10.** Nanobelt morphology typical of  $\text{H}_2\text{V}_3\text{O}_8$  prepared by 2 h microwave-hydrothermal route.

## 5. Conclusions

During this work, different technologically important complex oxides have been prepared by using microwave synthesis. It is clear that changing the conventional methodologies of inorganic synthesis to more environmental-friendly and cost effective methods, may help the development of a sustainable chemistry contributing to the preservation of the natural environment. Various microwave synthesis techniques have been employed: Solid state microwave synthesis, single-mode microwave synthesis and microwave-hydrothermal synthesis. Table 1 summarizes the three different methodologies.

The development of microwave synthesis for inorganic materials on a small scale in the laboratory has been demonstrated, but such techniques should also be further extended to industrial large scale production processes, which may pose certain challenges in terms of the reproducibility of such processes. Currently no equipment exists for large scale industrial production but the development of new apparatus is highly recommended.

**Table 1.** Summary of the microwave-synthesis techniques presented in this work.

Techniques	Reaction time	Temperature	Typical power	Pressure	Electromagnetic field defined in space	Irradiation modus	Crucible/vessel	Secondary heater	Plasma formation	Materials prepared in this work	Instrument prices
Solid-State Microwave	Fast ( $\approx 30$ min)	Difficult to control and measure	800 W	-	No	Multimode	Ceramic crucible	Black carbon	No	(1). $\text{LaTMO}_3$ (TM = Al, Cr, Mn, Fe, Co) and $\text{La}_{1-x}\text{Sr}_x\text{TMO}_3$ . (2). $(\text{RE})_2\text{Ti}_2\text{O}_7$ (RE = Rare Earth)	€
Single-Mode Microwave ( $\text{TE}_{10p}$ Microwave Cavity)	Very fast (<5 min)	Monitored with a pyrometer (>1400 °C)	100–200 W	-	Yes ( $\text{TE}_{10p}$ microwave cavity)	Single-mode	SiC crucible	SiC crucible	Sometimes	(1). $\text{Ba}_x\text{Mn}_8\text{O}_{16}$ . (2). $\text{LaCrO}_3$	€€€€€€€€€€
Microwave-Hydrothermal	Fast ( $\approx 30$ min)	Monitored with a T sensor (<230 °C)	500 W	Monitored with a P sensor (<100 bar)	No	Multimode	Vessel (Teflon, quartz)	Polar solvent	No	(1). $\text{RE}_x\text{CeO}_{2-d}$ . (2). $\text{H}_2\text{V}_3\text{O}_8$	€€€€€€€€€€

## Acknowledgments

The authors acknowledge funding from the Community of Madrid (Materyener3, S2013/MIT-2753) and the Ministry of Science and Innovation (MAT-2013-64452-C4-4-R). Rainer Schmidt acknowledges the Ministerio de Ciencia e Innovación (MICINN) for granting a Ramon y Cajal Fellowship. Many thanks for valuable contributions go to Sylvain Marinel (CRISMAT—CNRS), Ulises Amador and Alex Gomez (San Pablo CEU) and Beatriz Molero (University of Calgary).

## Author Contributions

All experimental work was carried out by J. Prado-Gonjal. The work was supervised by R. Schmidt and E. Morán. The paper was written by R. Schmidt, J. Prado-Gonjal and E. Morán.

## Conflicts of Interest

The authors declare no conflict of interest.

## References

1. Rouxel, J.; Tournoux, M. Chimie douce with solid precursors, past and present. *Solid State Ion.* **1996**, *84*, 141–149.
2. Schleich, D.M. Chimie douce: Low temperature techniques for synthesizing useful compounds. *Solid State Ion.* **1994**, *70–71*, 407–411.
3. Gopalakrishnan, J. Chimie Douce Approaches to the Synthesis of Metastable Oxide Materials. *Chem. Mater.* **1995**, *7*, 1265–1275.
4. Prado-Gonjal, J.; Schmidt, R.; Moran, E. Microwave Assisted Synthesis and Characterization of Perovskite Oxides. In *Perovskite: Crystallography, Chemistry and Catalytic Performance*; Zhang, J., Li, H., Eds.; Novascience Publishers: Hauppauge, NY, USA, 2014; pp. 117–140.
5. Prado-Gonjal, J.; Morán, E. Síntesis asistida por microondas de sólidos inorgánicos. *An. Quím.* **2011**, *107*, 129–136.
6. Cavani, F.; Centi, G.; Perathoner, S.; Trifirò, F. *Sustainable Industrial Chemistry*; John Wiley & Sons Ltd.: Hoboken, NJ, USA; 2009; p. 599.
7. Sheldon, R.A.; Arends, I.; Hanefeld, U. *Green Chemistry and Catalysis*; John Wiley & Sons Ltd.: Hoboken, NJ, USA; 2007.
8. Hutagalung, S.D.; Ibrahim, M.I.M.; Ahmad, Z.A. Microwave assisted sintering of  $\text{CaCu}_3\text{Ti}_4\text{O}_{12}$ . *Ceram. Int.* **2008**, *34*, 939–942.
9. Vaidhyanathan, B.; Raizada, P.; Rao, K.J. Microwave assisted fast solid state synthesis of niobates and titanates. *J. Mater. Sci. Lett.* **1997**, *16*, 2022–2025.
10. Prado-Gonjal, J.; Arevalo-Lopez, A.; Morán, E. Microwave-assisted synthesis: A fast and efficient route to produce  $\text{LaMO}_3$  ( $M = \text{Al, Cr, Mn, Fe, Co}$ ) perovskite materials. *Mater. Res. Bull.* **2011**, *46*, 222–230.

11. Prado-Gonjal, J.S.; Schmidt, R.; Romero, J.-J.; Ávila, D.; Amador, U.; Morán, E. Microwave-Assisted Synthesis, Microstructure, and Physical Properties of Rare-Earth Chromites. *Inorg. Chem.* **2012**, *52*, 313–320.
12. Prado-Gonjal, J.; Schmidt, R.; Ávila, D.; Amador, U.; Morán, E. Structural and physical properties of microwave synthesized orthorhombic perovskite erbium chromite  $\text{ErCrO}_3$ . *J. Eur. Ceram. Soc.* **2012**, *32*, 611–618.
13. Schmidt, R.; Prado-Gonjal, J.; Ávila, D.; Amador, U.; Morán, E. Electron microscopy of microwave-synthesized rare-earth chromites. In *Microscopy: Advances in Scientific Research and Education*; Mendez-Vilas, A., Ed.; Formatex Research Center: Badajoz, Spain, 2014; Microscopy Book Series #6, pp. 819–826.
14. Ragupathy, P.; Vasan, H.N.; Munichandraiah, N. Microwave driven hydrothermal synthesis of  $\text{LiMn}_2\text{O}_4$  nanoparticles as cathode material for Li-ion batteries. *Mater. Chem. Phys.* **2010**, *124*, 870–875.
15. Yan, H.; Huang, X.; Chen, L. Microwave synthesis of  $\text{LiMn}_2\text{O}_4$  cathode material. *J. Power Sources* **1999**, *81–82*, 647–650.
16. Lu, X.; Ding, Y.; Dan, H.; Yuan, S.; Mao, X.; Fan, L.; Wu, Y. Rapid synthesis of single phase  $\text{Gd}_2\text{Zr}_2\text{O}_7$  pyrochlore waste forms by microwave sintering. *Ceram. Int.* **2014**, *40*, 13191–13194.
17. Bonamartini Corradi, A.; Bondioli, F.; Ferrari, A.M.; Manfredini, T. Synthesis and characterization of nanosized ceria powders by microwave-hydrothermal method. *Mater. Res. Bull.* **2006**, *41*, 38–44.
18. Bondioli, F.; Ferrari, A.M.; Lusvardi, L.; Manfredini, T.; Nannarone, S.; Pasquali, L.; Selvaggi, G. Synthesis and characterization of praseodymium-doped ceria powders by a microwave-assisted hydrothermal (MH) route. *J. Mater. Chem.* **2005**, *15*, 1061–1066.
19. Prado-Gonjal, J.; Molero-Sánchez, B.; Ávila-Brandé, D.; Morán, E.; Pérez-Flores, J.C.; Kuhn, A.; García-Alvarado, F. The intercalation chemistry of  $\text{H}_2\text{V}_3\text{O}_8$  nanobelts synthesised by a green, fast and cost-effective procedure. *J. Power Sources* **2013**, *232*, 173–180.
20. Bazuev, G.V.; Tyutyunnik, A.P.; Berger, I.F.; Nikolaenko, I.V.; Golovkin, B.G. Microwave synthesis, structure, and magnetic properties of quasi-one-dimensional complex oxide  $\text{Sr}_4\text{LiMn}_2\text{O}_9$ . *J. Alloy. Compd.* **2011**, *509*, 6158–6162.
21. Valan, M.F.; Manikandan, A.; Antony, S.A. Microwave Combustion Synthesis and Characterization Studies of Magnetic  $\text{Zn}_{1-x}\text{Cd}_x\text{Fe}_2\text{O}_4$  ( $0 \leq x \leq 0.5$ ) Nanoparticles. *J. Nanosci. Nanotechnol.* **2015**, *15*, 4543–4551.
22. Sonia; Patel, R.K.; Kumar, P.; Prakash, C.; Agrawal, D.K. Low temperature synthesis and dielectric, ferroelectric and piezoelectric study of microwave sintered  $\text{BaTiO}_3$  ceramics. *Ceram. Int.* **2012**, *38*, 1585–1589.
23. Komarneni, S.; Li, Q.; Stefansson, K.M.; Roy, R. Microwave-hydrothermal processing for synthesis of electroceramic powders. *J. Mater. Res.* **1993**, *8*, 3176–3183.
24. Prado-Gonjal, J.; Villafuerte-Castrejón, M.; Fuentes, L.; Moran, E. Microwave-hydrothermal synthesis of the multiferroic  $\text{BiFeO}_3$ . *Mater. Res. Bull.* **2009**, *44*, 1734–1737.
25. Prado-Gonjal, J.; Ávila, D.; Villafuerte-Castrejón, M.; González-García, F.; Fuentes, L.; Gómez, R.; Pérez-Mazariego, J.; Marquina, V.; Morán, E. Structural, microstructural and Mössbauer study of  $\text{BiFeO}_3$  synthesized at low temperature by a microwave-hydrothermal method. *Solid State Sci.* **2011**, *13*, 2030–2036.

26. Birkel, C.S.; Zeier, W.G.; Douglas, J.E.; Lettiere, B.R.; Mills, C.E.; Seward, G.; Birkel, A.; Snedaker, M.L.; Zhang, Y.; Snyder, G.J.; *et al.* Rapid Microwave Preparation of Thermoelectric TiNiSn and TiCoSb Half-Heusler Compounds. *Chem. Mater.* **2012**, *24*, 2558–2565.
27. Biswas, K.; Muir, S.; Subramanian, M.A. Rapid microwave synthesis of indium filled skutterudites: An energy efficient route to high performance thermoelectric materials. *Mater. Res. Bull.* **2011**, *46*, 2288–2290.
28. Bhat, M.H.; Chakravarthy, B.P.; Ramakrishnan, P.A.; Levasseur, A.; Rao, K.J. Microwave synthesis of electrode materials for lithium batteries. *Bull. Mater. Sci.* **2000**, *23*, 461–466.
29. Prado-Gonjal, J.; Schmidt, R.; Espíndola-Canuto, J.; Ramos-Alvarez, P.; Morán, E. Increased ionic conductivity in microwave hydrothermally synthesized rare-earth doped ceria  $Ce_{1-x}RE_xO_{2-(x/2)}$ . *J. Power Sources* **2012**, *209*, 163–171.
30. Kingston, H.M.; Haswell, S.J. *Microwave-Enhanced Chemistry: Fundamentals, Sample Preparation, and Applications*; American Chemical Society: Washington, DC, USA; 1997; p. 772.
31. Gupta, M.; Leong, E.W.W. *Microwaves and Metals*; John Wiley & Sons (Asia) Pte. Ltd.: Singapore, Singapore; 2008; p. 228.
32. Clark, D.E.; Folz, D.C.; West, J.K. Processing materials with microwave energy. *Mater. Sci. Eng. A* **2000**, *287*, 153–158.
33. Tao, S.; Irvine, J.T.; Kilner, J.A. An Efficient Solid Oxide Fuel Cell Based upon Single-Phase Perovskites. *Adv. Mater.* **2005**, *17*, 1734–1737.
34. Petrovic, S.; Terlecki-Baricevic, A.; Karanovic, L.; Kirilov-Stefanov, P.; Zdujic, M.; Dondur, V.; Paneva, D.; Mitov, I.; Rakic, V.  $LaMO_3$  ( $M = Mg, Ti, Fe$ ) perovskite type oxides: Preparation, characterization and catalytic properties in methane deep oxidation. *Appl. Catal. B* **2008**, *79*, 186–198.
35. Hong, W.T.; Stoerzinger, K.A.; Moritz, B.; Devereaux, T.P.; Yang, W.; Shao-Horn, Y. Probing  $LaMO_3$  Metal and Oxygen Partial Density of States Using X-ray Emission, Absorption, and Photoelectron Spectroscopy. *J. Phys. Chem. C* **2015**, *119*, 2063–2072.
36. Vázquez-Vázquez, C.; Kögerler, P.; López-Quintela, M.A.; Sánchez, R.D.; Rivas, J. Preparation of  $LaFeO_3$  particles by sol-gel technology. *J. Mater. Res.* **1998**, *13*, 451–456.
37. Krupicka, E.; Reller, A.; Weidenkaff, A. Morphology of nanoscaled  $LaMO_3$ -particles ( $M = Mn, Fe, Co, Ni$ ) derived by citrate precursors in aqueous and alcoholic solvents. *Cryst. Eng.* **2002**, *5*, 195–202.
38. Rida, K.; Benabbas, A.; Bouremmad, F.; Peña, M.A.; Sastre, E.; Martínez-Arias, A. Effect of calcination temperature on the structural characteristics and catalytic activity for propene combustion of sol-gel derived lanthanum chromite perovskite. *Appl. Catal. A* **2007**, *327*, 173–179.
39. Najjar, H.; Batis, H. La-Mn perovskite-type oxide prepared by combustion method: Catalytic activity in ethanol oxidation. *Appl. Catal. A* **2010**, *383*, 192–201.
40. Subramanian, M.A.; Aravamudan, G.; Subba Rao, G.V. Oxide pyrochlores: A review. *Prog. Solid State Chem.* **1983**, *15*, 55–143.
41. Greedan, J.E. Geometrically Frustrated Magnetic Materials. In *Functional Oxides*; Bruce, D.W., O'Hare, D., Walton, R.I., Eds.; John Wiley & Sons Ltd.: Hoboken, NJ, USA; 2011; pp. 41–117.



42. Brixner, L.H. Preparation and Properties of the  $\text{Ln}_2\text{Ti}_2\text{O}_7$ -Type Rare Earth Titanate. *Inorg. Chem.* **1964**, *3*, 1065–1067.
43. Kitchen, H.J.; Vallance, S.R.; Kennedy, J.L.; Tapia-Ruiz, N.; Carassiti, L.; Harrison, A.; Whittaker, A.G.; Drysdale, T.D.; Kingman, S.W.; Gregory, D.H.; *et al.* Modern Microwave Methods in Solid-State Inorganic Materials Chemistry: From Fundamentals to Manufacturing. *Chem. Rev.* **2014**, doi:10.1021/cr4002353.
44. Katsuki, H.; Furuta, S.; Komarneni, S. Semi-continuous and fast synthesis of nanophase cubic  $\text{BaTiO}_3$  using a single-mode home-built microwave reactor. *Mater. Lett.* **2012**, *83*, 8–10.
45. Cheng, J.; Roy, R.; Agrawal, D. Radically different effects on materials by separated microwave electric and magnetic fields. *Mater. Res. Innov.* **2002**, *5*, 170–177.
46. Roy, R.; Pelemedu, R.; Hurtt, L.; Cheng, J.; Agrawal, D. Definitive experimental evidence for Microwave Effects: Radically new effects of separated E and H fields, such as decrystallization of oxides in seconds. *Mater. Res. Innov.* **2002**, *6*, 128–140.
47. Vetl, G.; Petzoldt, F.; Pueschner, P.A. Effects of microwave on sintering processes. In Proceedings of the Euro PM 2004 World Congress, Vienna, Austria, 17–21 October 2004; EMPA: Vienna, Austria, 2004.
48. Ishiwata, S.; Bos, J.W.G.; Huang, Q.; Cava, R.J. Structure and magnetic properties of hollandite  $\text{Ba}_{1.2}\text{Mn}_8\text{O}_{16}$ . *J. Phys. Condens. Matter* **2006**, *18*, 3745.
49. Nistor, L.C.; van Tendeloo, G.; Amelinckx, S. Defects and Phase Transition in Monoclinic Natural Hollandite:  $\text{Ba}_x\text{Mn}_8\text{O}_{16}$ . *J. Solid State Chem.* **1994**, *109*, 152–165.
50. Boroomand, F.; Wessel, E.; Bausinger, H.; Hilpert, K. Correlation between defect chemistry and expansion during reduction of doped  $\text{LaCrO}_3$  interconnects for SOFCs. *Solid State Ion.* **2000**, *129*, 251–258.
51. Feng, S.; Li, G. Hydrothermal and Solvothermal Syntheses. In *Modern Inorganic Synthetic Chemistry*; Elsevier B.V.: Amsterdam, The Netherlands; 2011; pp. 63–93.
52. Komarneni, S.; Roy, R.; Li, Q.H. Microwave-hydrothermal synthesis of ceramic powders. *Mater. Res. Bull.* **1992**, *27*, 1393–1405.
53. Komarneni, S.; D'Arrigo, M.C.; Leonelli, C.; Pellacani, G.C.; Katsuki, H. Microwave-Hydrothermal Synthesis of Nanophase Ferrites. *J. Am. Ceram. Soc.* **1998**, *81*, 3041–3043.
54. Maricle, D.; Swarr, T.; Karavolis, S. Enhanced ceria—A low-temperature SOFC electrolyte. *Solid State Ion.* **1992**, *52*, 173–182.
55. Ali, S.M.; Rosli, R.E.; Muchtar, A.; Sulong, A.B.; Somalu, M.R.; Majlan, E.H. Effect of sintering temperature on surface morphology and electrical properties of samarium-doped ceria carbonate for solid oxide fuel cells. *Ceram. Int.* **2015**, *41*, 1323–1332.